www.czasopisma.pan.pl PAN POLSKA AKADEMIA NAUK www.journals.pan.pl

Metrol. Meas. Syst., Vol. XX (2013), No. 4, pp. 689–696.

PAN POLSKA AKADEMIA NAUK

METROLOGY AND MEASUREMENT SYSTEMS

Index 330930, ISSN 0860-8229

www.metrology.pg.gda.pl

M&MS

COUPLED ENERGY MEASUREMENTS IN MULTI-CORE PHOTONIC-CRYSTAL FIBERS

Jacek Klimek

Maria Curie-Sklodowska University, Faculty of Chemistry, Laboratory of Optical Fibers Technology, Sklodowska Sq. 3, 20-031 Lublin, Poland (✉ jacek.klimek@umcs.pl)

Abstract

This paper outlines a measurement method of properties of microstructured optical fibers that are useful in sensing applications. Experimental studies of produced photonic-crystal fibers allow for a better understanding of the principles of energy coupling in photonic-crystal fibers. For that purpose, fibers with different filling factors and lattice constants were produced. The measurements demonstrated the influence of the fiber geometry on the coupling level of light between the cores. For a distance between the cores of 15 µm, a very low level (below 2%) of energy coupling was obtained. For a distance of 13 µm, the level of energy transfer to neighboring cores on the order of 2-4% was achieved for a filling factor of 0.29. The elimination of the energy-coupling phenomenon between the cores was achieved by duplicating the filling factor of the fiber. The coupling level was as high as 22% in the case of fibers with a distance between the cores of 8.5 µm. Our results can be used for microstructured-fiber sensing applications and for transmission-channel switching in liquid-crystal multi-core photonic fibers.

Keywords: photonic-crystal fibers, multi-core fibers, optical-fiber measurements, photonic sensors.

1. Introduction

The propagation of light in multi-core microstructured optical fibers is strongly determined by their structure. Such fibers are used as sensors for many non-electrical quantities [1]. At present, their birefringence and their ability to operate in optical-fiber interferometer systems are often exploited [2]. For the past few years, photonic-crystal fibers (PCF) have been used as pressure, strain, stress and deflection sensors and in many chemical sensors [3]. PCF structures for high-sensitivity sensing are also demonstrated [4-5]. Studies focused on the possibility of using optical-fiber sensors at varying temperatures have also been conducted [6].

It is important that sensors based on photonic-crystal fibers utilize the phenomenon of the coupling-length change between fiber cores. This change is dependent on the magnitude of the measured value. It is therefore important to determine the energy coupling level between the photonic-crystal fiber cores in a specific measuring system for the particular geometry of the fiber. It is also important to determine the influence of the fiber geometry on the energy coupling level between microstructured fiber cores.

Most often, the distances between considered fiber cores are sufficiently large to allow the reduction of the phenomenon of coupling energy between the cores. On the other hand, large distances between the cores limit the total number of cores that can be used and cause problems for the manufacture of the fibers. Many studies of the energy coupling between modes of multimode fibers and between two cores in photonic-crystal fibers have been conducted. These studies, however, are limited to cases in which the transfer involves similar values of the normalized frequencies of the cores.

Article history: received on Jun. 29, 2013; accepted on Oct. 26, 2013; available online on Dec. 10, 2013; DOI: 10.2478/mms-2013-0059.

In this paper, the problem of energy coupling in microstructured optical fibers consisting of ten cores is presented. The proposed fibers have significantly different values of normalized frequency in each core. The energy coupling level between the cores was measured, and image processing was utilized. The presented measurement results are also important for transmission-channel switching, particularly in photonic-crystal fiber systems with a large number of cores [7]. A compact multi-core fiber laser for phase locking and in-phase supermode selection as well as the phase-locked operation of a multi-emitter laser device have also been demonstrated in the literature [8].

The results presented in this article concern measurements of the energy coupling between cores of specially designed and manufactured fibers. For this purpose, fibers with various filling factors and the same core configuration were prepared. The measurement results demonstrated the influence of the fiber geometry on the light coupling level between cores. Appropriate analysis of the experimentally obtained images allowed the accurate determination of the percentage level of the energy coupling and provided an opportunity to determine the influence of the fiber geometry. The results indicate that to understand the problem of light coupling in an optical-fiber structure, it is necessary to use a modeling method for light propagation, such as the finite element method, which is also used for modeling the response to measurands that affect the optical fibers [9].

2. Methodology for measuring the level of energy coupling between the microstructured-fiber cores

Measurements were performed in a system that enabled the selective stimulation of the cores and allowed the image registration of the input and output surfaces of the designed fibers, as shown in Figure 1.

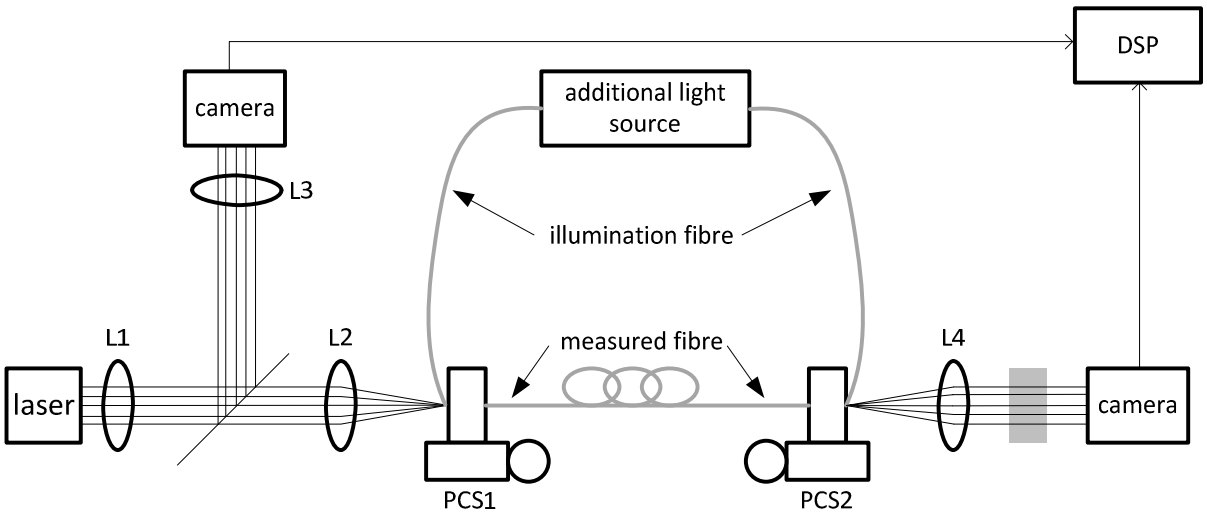

Fig. 1. The measurement system for measuring the level of energy coupling between the microstructured-fiber cores.

The measurements relied on selectively introducing HeNe laser light into the selected microstructured-fiber core. The selective stimulation of specific fiber cores was achieved by the arrangement of the observation system for the input face of the fiber and control of the light-spot location. After passing through lenses L1 and L2, the laser light (633 nm) was focused on the fiber face using Position Control System PCS1, which allowed rotation and three-axis linear adjustment of the position of the front of the fiber. The size of the focused

Metrol. Meas. Syst., Vol. XX (2013), No. 4, pp. 689–696.

light spot was 4 μm. This value ensured the coverage of the entire surface of one of the cores in all manufactured fibers. The portion of the light that was reflected from the fiber input after passing through lens L2 was directed to the beam splitter and was focused using the L3 lens onto the camera, which was equipped with a charge-coupled device. The GP-KR222 1/2" digital signal processing camera has been used which features a second generation DSP chip. The GP-KR222 incorporates a 1/2" interline transfer CCD (380,000 pixels: effective) with a micro lens on each pixel which achieves high sensitivity of 3 lux at F1.4, outstanding 480-line horizontal resolution, and signal-to-noise ratio of 50dB. Both fiber ends were additionally lighted to obtain favorable imaging conditions for the cameras. For this purpose the halogen medical iluminator Dentalux Lumed and plastic-clad silica fibers PCS 600 (600 μm of diameter) have been used. After passing through 35 meters of microstructured fiber, the light signal was then directed to the L4 lens, a neutral density filter and the camera that recorded the output face of the fiber. For effective imaging, PCS2 permitted the position adjustment of the output face of the fiber. The signals from the camera were then analyzed in the MATLAB environment, which allowed the determination of the percentage value of the power coupling between the cores of the manufactured fibers. The numerical analysis of the obtained images required the signal gain of the camera to remain constant. Therefore, it was necessary to disable the automatic gain control, which in turn resulted in camera saturation. The use of a neutral density filter with selected attenuation allowed the elimination of the camera-saturation effect and the recording the correct signals. Figure 2 shows cross-sectional images of the fibers, which were obtained using a scanning electron microscope (SEM).

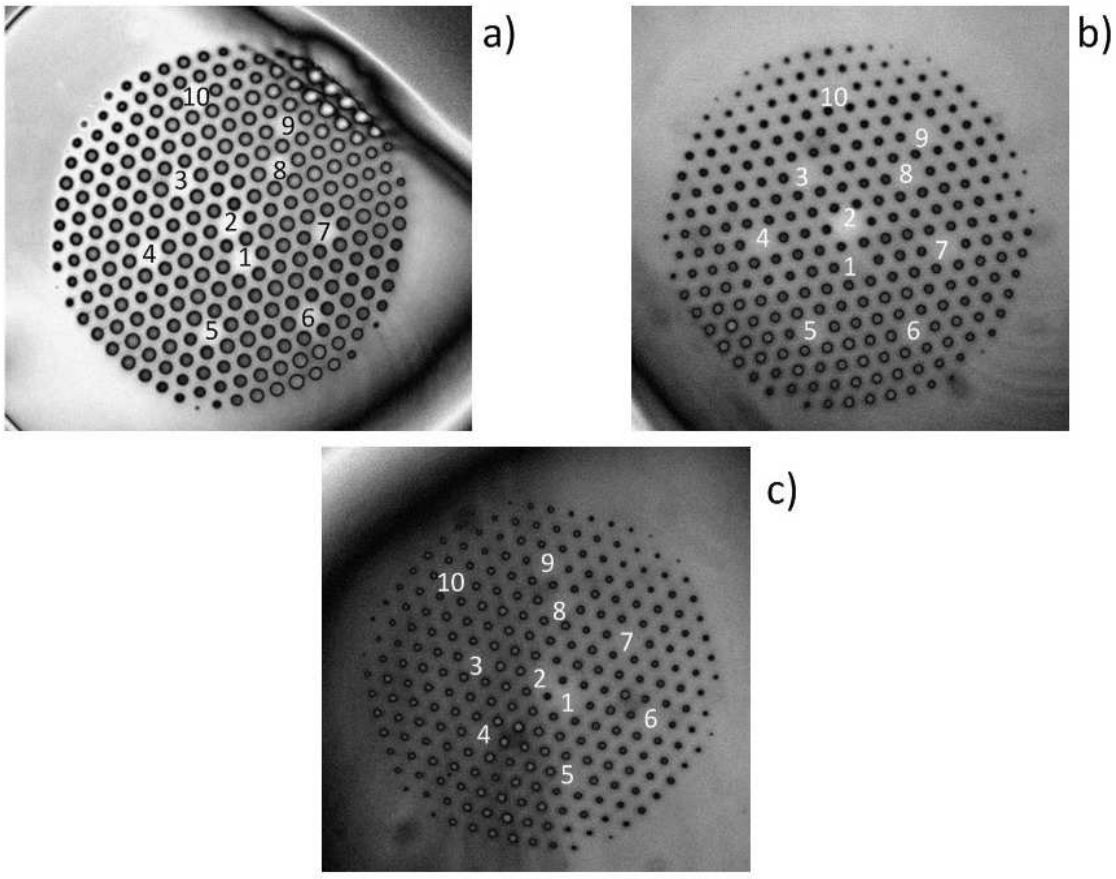

Fig. 2. Images of the investigated photonic-crystal fibers obtained with a scanning electron microscope. The cores are marked with numbers.

For the purpose of the energy-coupling analysis, the cores were assigned numbers using the scheme shown in Figure 2. The filling factors were 0.68, 0.45 and 0.29, respectively, for the fibers shown in 2a), 2b) and 2c). Measurements of the distances between the cores were also performed. The distances between the cores are summarized in Table 1. The table shows only the distances corresponding to the cores between which the energy coupling was observed.

Table 1. The distances between selected fiber cores.

Cores	Distance defined in terms of the lattice constant	Distance for fiber a) [μm]	Distance for fiber b) [μm]	Distance for fiber c) [μm]
1 to 2	0.5 Λ	2.35	2.00	2.08
8 to 9	1.0 Λ	4.70	4.00	4.15
2 to 3	2.0 Λ	9.40	8.00	8.30
3 to 4	2.5 Λ	11.75	10.00	10.38
4 to 5	3.5 Λ	16.45	14.00	14.53
1 to 7	3.0 Λ	14.10	12.00	12.45

3. Results and analysis of the energy-coupling measurements

Figure 3 is a graph of normalized light intensity that was produced in the MATLAB environment based on images from the CCD camera. The pictured results concern the fiber with a filling factor of 0.68.

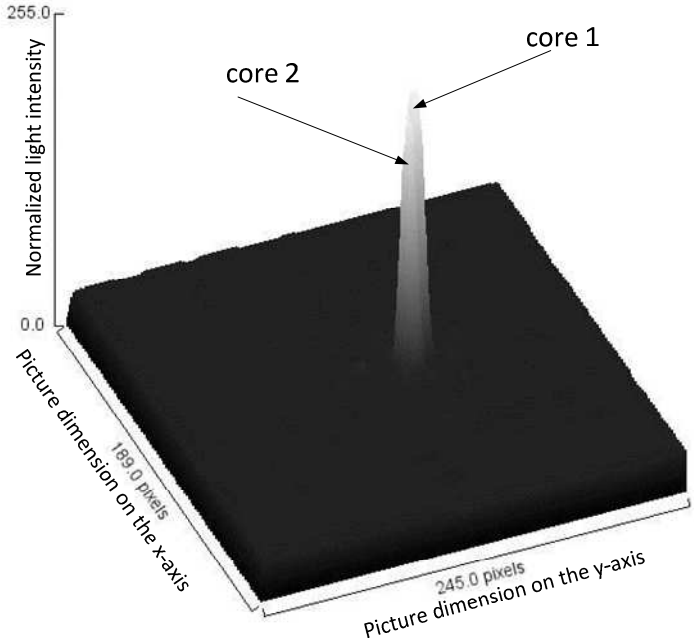

Fig. 3. Intensity graph of the output-plane signal of a photonic-crystal fiber. Lattice constant: Λ = 4.7 μm; core diameter: d = 3.2 μm; filling factor: 0.68; number of stimulated cores: 1.

The core numbers are marked in Figure 3. Similar results for the other values of the fiber filling factor are shown in Figure 4 (filling factor of 0.45) and Figure 5 (filling factor of 0.29).

Metrol. Meas. Syst., Vol. XX (2013), No. 4, pp. 689–696.

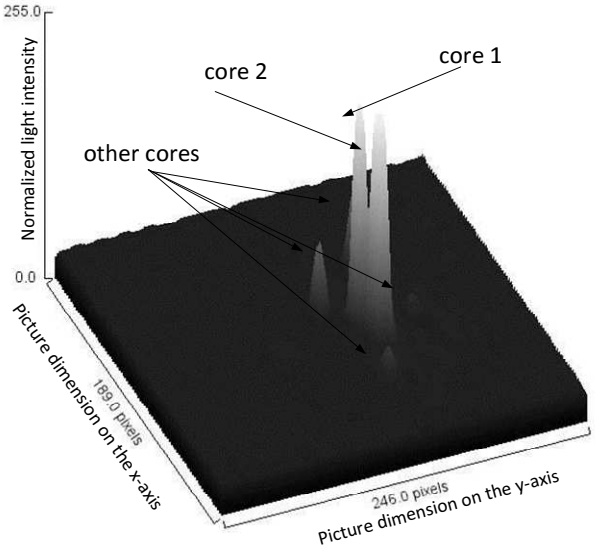

Fig. 4. Intensity graph of the output-plane signal of a photonic-crystal fiber. Lattice constant: $\Lambda = 4$ µm; core diameter: d = 1.6 µm; filling factor: 0.45; number of stimulated cores: 1.

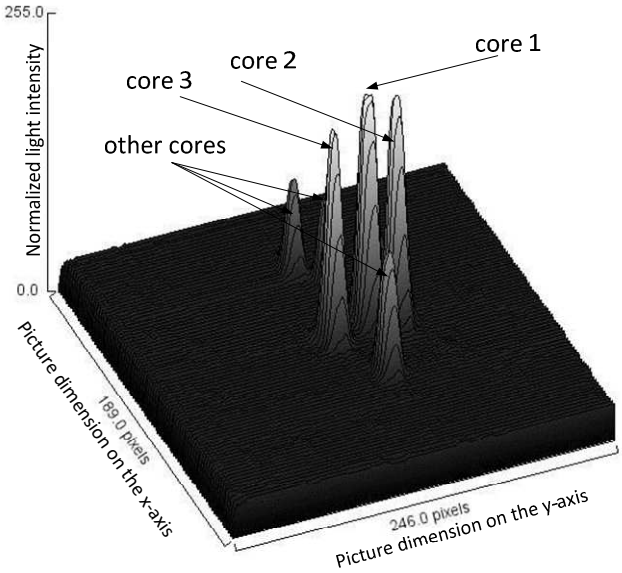

Fig. 5. Intensity graph of the output-plane signal of a photonic-crystal fiber. Lattice constant: $\Lambda = 4.15$ µm; core diameter: d = 1.2 µm; filling factor: 0.29; number of stimulated cores: 1.

The energy transfers between the cores of the fibers were determined based on the data obtained from the cameras. Digital signal processing allowed the determination of the percentages of the light signals that propagated in non-stimulated cores. The percentages were determined by comparison to the maximum power value obtained for a given stimulation. The results are presented in Figures 6-8.

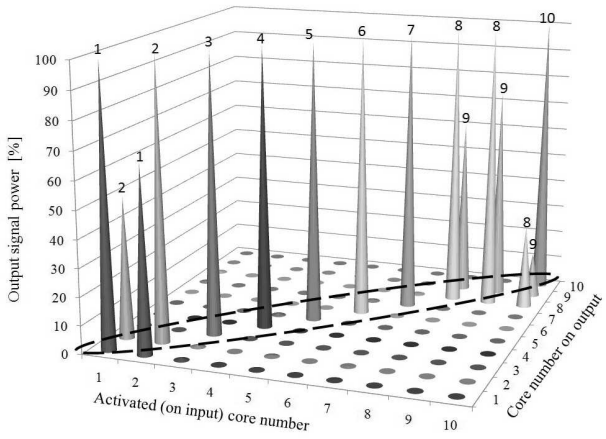

Fig. 6. The percentage of the output power carried by each core determined on the basis of camera images of the end of the fiber. Lattice constant: Λ = 4.7 μm; core diameter: d = 3.2 μm; filling factor: 0.68.

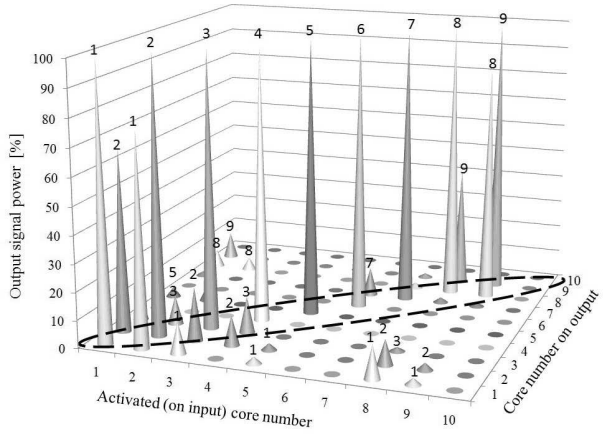

Fig. 7. The percentage of the output power carried by each core determined on the basis of camera images of the end of the fiber. Lattice constant: Λ = 4 μm; core diameter: d = 1.6 μm; filling factor: 0.45.

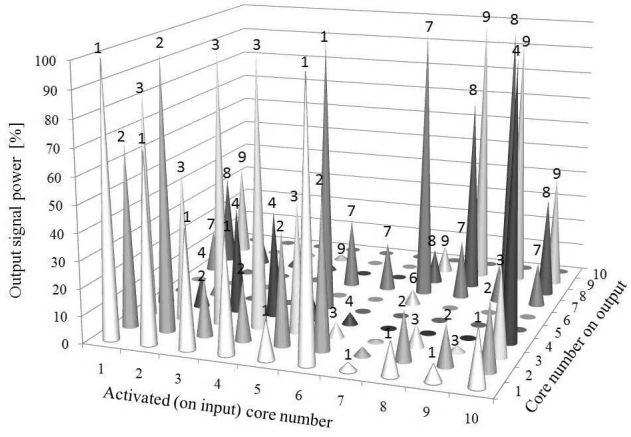

Fig. 8. The percentage of the output power carried by each core determined on the basis of camera images of the end of the fiber. Lattice constant: Λ = 4.15 μm; core diameter: d = 1.2 μm; filling factor: 0.29.

Metrol. Meas. Syst., Vol. XX (2013), No. 4, pp. 689–696.

The maximum percentage of the output power for the fibers with filling factors of 0.45 (Fig. 7) and 0.68 (Fig. 6) is carried by the core into which the signal was introduced at the input face of the fiber. The area characterized by the maximum output power is marked in Figures 6 and 7. This area corresponds to the cores that were stimulated in each measurement. In addition to the main signal in the core that was stimulated, energy coupling to the other cores can be observed. In both cases (Figures 6 and 7), the highest power leakages occurred between core 1 and core 2 and between core 8 and core 9. Below a certain value of the filling factor, a considerable increase in the phenomenon of power coupling to the other cores appears, as shown clearly in Figure 8. When the filling factor is relatively small, couplings to more cores appear because of the smaller distances between the cores.

4. Summary

The measurements demonstrated the ability to control the level of energy coupling between cores, because the amount of energy coupling between cores decreases as the filling factor of the fiber increases. When the obtained results and the fiber geometries were analyzed, it was found that the level of energy coupling between the cores decreases as the distance between the cores increases.

This study has also confirmed that it is possible to quantify the energy coupling by analysis of the signals obtained from a CCD camera. Cores located closer to the edge of the structure are weakly guided cores. The least guided core in this study was core number 10, as it was situated at a distance of 9 microns from the edge of the structure. The energy carried by that core easily escaped the fiber structure.

For distances between the cores on the order of 15 μm, the level of energy coupling was below 2%. For distances of 13 μm, the level of coupling to adjacent cores had a value of 2-4% for a fiber filling factor of 0.29, and it decreased to 0 for a fiber filling factor of 0.45. In the case in which the distance between the cores was on the order of 8.5 μm, the coupling level was 22%.

The results indicate that for each core, the distance to the next nearest core determines its single-mode operation. For example, the best guided core was core number 7. The distance to the nearest core was 11 μm, which caused the fiber to behave almost like a single-core fiber when core 7 was activated.

In the investigated fiber structures, the unique determination of the coupling paths among the cores is a difficult issue because the energy transfer between cores 7 and 8 may be performed by cores 4, 2, 1, and 5 or by cores 4 and 5. Therefore, it seems reasonable to further pursue this work using methods that allow numerical calculations of the light propagation in the microstructured fibers. The results indicate that to understand the problem of light propagation in the investigated fiber structures, it is necessary to use methods of fiber modeling [10]. Examples of modeling methods include the beam propagation method (BPM), the finite-difference vector beam propagation method (FD-VBPM), the lines method, and the multipole method. It is also possible to use plane-wave method modeling [11], which is used in optics to solve light-scattering problems [12-15]. Such modeling can be implemented numerically or in a hybrid way, using analytical methods.

5. References

[1] Statkiewicz, G., Martynkien, T., Urbańczyk, W. (2004). Measurements of modal birefringence and polarimetric sensitivity of the birefringent holey fiber to hydrostatic pressure and strain. *Optics Communications*, 241(4–6), 339–348.

[2] Wójcik, J., Makara, M., Mergo, P., Janoszczyk, B., Klimek, J. (2006). Microstructured low and high birefringence four core fibers for sensing applications. *Proc. SPIE*, 6189, 61890B.

[3] Frazão, O., Santos, J.L., Araújo, F.M., Ferreira, L.A. (2008). Optical sensing with photonic crystal fibers. *Laser and Photonics Reviews*, 2(6), 449–459.

[4] Favero, F.C., Araujo, L., Bouwmans, G., Finazzi, V., Villatoro, J., Pruneri, V. (2012). Spheroidal Fabry-Perot microcavities in optical fibers for high-sensitivity sensing. *Optics Express*, 20(7), 7112-7118.

[5] Pinto, A.M.R., Lopez-Amo, M. (2012). Photonic Crystal Fibers for Sensing Applications. *Journal of Sensors*, art. no. 598178, 1–21.

[6] Kisała, P. (2013). Measurement of the maximum value of non-uniform strain using a temperature-insensitive fibre Bragg grating method. *Opto-electronics Review*, (21)3, 293–302.

[7] Woliński, T.R., Szaniawska, K., Ertman, S., Lesiak, P., Domański, A.W., Dąbrowski, R., Nowinowski-Kruszelnicki, E., Wójcik, J. (2006). Influence of temperature and electrical fields on propagation properties of photonic liquid-crystal fibers. *Meas. Sci. Technol*, 17, 985–991.

[8] Li, L., Schülzgen, A., Chen, S., Temyanko, V.L., Moloney, J.V., Peyghambarian, N. (2006). Phase locking and in-phase supermode selection in monolithic multicore fiber lasers. *Opt. Lett*., 31, 2577–2579.

[9] Kisała, P. (2012). Application of inverse analysis to determine the strain distribution with optoelectronic method insensitive to temperature changes. *Applied Optics*, (51)16, 3599–3604.

[10] Mroczka, J. (2013). The cognitive process in metrology. *Measurement*, 46, 2896–2907.

[11] Mroczka, J., Wysoczański, D. (2000). Plane-wave and Gaussian-beam scattering on an infinite cylinder. *Optical Engineering*, 39(3), 763–770.

[12] Girasole, T. Le Toulouzan, J. N., Mroczka, J., Wysoczanski, D. (1997). Fiber orientation and concentration analysis by light scattering: Experimental setup and diagnosis. *Review of Scientific Instruments*, 68(7), 2805–2811.

[13] Girasole, T., Bultynck, H., Gouesbet, G., Gréhan, G., Le Meur, F., Le Toulouzan, J.N., Mroczka, J., Ren, K.F., Rozé, C., Wysoczanski, D. (1997). Cylindrical fibre orientation analysis by light scattering. Part 1: Numerical aspects. *Particle and Particle Systems Characterization*, 14(4), 163–174.

[14] Girasole, T., Gouesbet, G., Gréhan, G., Le Toulouzan, J.N., Mroczka, J., Ren, K.F., Wysoczanski, D. (1997). Cylindrical fibre orientation analysis by light scattering. Part 2: Experimental aspects. *Particle and Particle Systems Characterization*, 14(5), 211–218.

[15] Mroczka, J. Szczuczyński, D. (2013). Improved technique of retrieving particle size distribution from angular scattering measurements. Journal of Quantitative Spectroscopy and Radiative Transfer, http://dx.doi.org/10.1016/j.jqsrt.2013.05.030.